의학석사 학위논문

Alterations of CD103$^+$ dendritic cells in autoimmune dry eye murine model

자가면역성 건성안 쥐모델에서의 CD103$^+$ 수지상 세포의 분포 변화

2021년 8월

서울대학교 대학원
의학과 안과학 전공
정 영 호

Alterations of CD103$^+$ dendritic cells in autoimmune dry eye murine model

자가면역성 건성안 쥐모델에서의 CD103$^+$ 수지상 세포의 분포 변화

지도 교수 김 미 금

이 논문을 의학석사 학위논문으로 제출함

2021년 4월

서울대학교 대학원
의학과 안과학 전공
정 영 호

정영호의 의학석사 학위논문을 인준함

2021년 7월

위 원 장 현 준 영

부위원장 김 미 금

위 원 송 현 범

Abstract

Alterations of $CD103^+$ dendritic cells in autoimmune dry eye murine model

Young Ho Jung

Ophthalmology

The Graduate School of Medicine

Seoul National University

Purpose : We aimed to investigate whether changes in antigen-presenting cell (APC) distributions are distinct in aging-dependent and autoimmune dry eye model.

Methods : Corneal staining and tear secretion were evaluated in 8-week- and 20-month-old C57BL/6 (B6) mice and 5-week- and 24-week-old NOD.B10.H2b mice. In the cornea, lacrimal gland (LG), and mesenteric lymph node, MHC-II^{hi} B cells ($CD45^+CD11b^-CD11c^-CD24^+$MHC-$II^{hi}$), $CD11b^-$ dendritic cells (DCs) ($CD45^+CD11b^-CD11c^+CD24^+$MHC-$II^{hi}$), $CD11b^+$DCs ($CD45^+CD11b^+CD11c^+CD24^+$MHC-$II^{hi}$), and $CD103^+$ DCs ($CD45^+CD11b^{+/-}CD11c^+CD103^+$MHC-$II^{hi}$) were compared between young and aged mice. Changes of fecal bacterial genomic 16S rRNA sequences were compared.

Results: Corneal staining increased, but tear secretion decreased in both aged mice ($P<0.001$). In aged B6 mice, the percentage of corneal $CD11b^+$ DCs was higher ($P<0.05$) than that in young mice. The percentages of mesenteric $CD11b^+$ DCs and $CD103^+CD11b^+$ DCs in the aged mice were higher than those in young mice ($P<0.05$). In aged NOD.B10.H2b mice, the percentages of corneal $CD103^+CD11b^-$ DCs and MHC-II^{hi} B cells in the LG were higher than those in young mice ($P<0.05$). The percentages of mesenteric $CD103^+CD11b^+$ DCs, $CD103^+CD11b^-$ DCs and MHC-II^{hi} B cells were also higher than those in young mice ($P<0.05$). α-diversity increased in aged B6 mice. β-diversity showed a significant difference between aged and young mice ($P<0.05$). In the aged B6 mice, nine taxa in the family *Lachnospiraceae* increased, while eight taxa in the family *Lactobacillaceae* decreased.

Conclusion: Gut-related $CD103^+CD11b^-$ DCs and MHC-II^{hi} B cells may be prevalent in aged autoimmune dry eye models, while $CD103^+$ DCs are not predominant in aging-dependent dry eye model.

Keywords : Autoimmune disease, dendritic cells (DCs), antigen-presenting cell (APC), dry eye, CD103 DC, MHC-II^{hi} B cell

Student Number : 2016-21948

Contents

LIST OF TABLES AND FIGURES

LIST OF ABBREVIATIONS

DC, dendritic cell

Treg, regulatory T cell

APC, antigen presenting cell

DED, dry eye disease

LG, lacrimal gland

NOD, NOD(Non obese diabetic).B10.H2b

B6, C57BL/6

IACUC, institutional Animal Care and Use Committee

ARVO, association for Research in Vision and Ophthalmology

ARRIVE, animal Research: Reporting of In Vivo Experiments

NEI, national Eye Institute

Co, cornea

MLN, mesenteric lymph node

MHC, major histocompatibility complex

FBS, fetal bovine serum

MQ, macrophage

BW, body weight

OTU, operational taxonomic units

LEfSe, linear discriminant analysis effect size

LDA, linear discriminant analysis

IFN, interferon

cDC, conventional dendritic cell

Th, T helper

1. Introduction

Since Ralph Steinman and Zanvil Cohn discovered the dendritic cell (DC),[1] DCs have been studied as key mediators of innate and adaptive immunity.[2, 3] DCs can also activate regulatory T cells (Treg) and tolerize T cells to self-antigens.[4, 5] Thus, DCs are being studied for their potential therapeutic benefits against autoimmune diseases.[6] Specific DC subset functions change during aging or in a tissue-specific manner, and a breakdown in the balance between functions may lead to autoimmune diseases.[7] Therefore, changes in DCs during aging should be studied.

DCs are found both in lymphoid and in non-lymphoid organs such as the skin, muscle, lung, kidney, intestine, liver, and eye and each organ has different primary antigen presenting cells (APC).[1, 2, 8-12]

Table 1. Major antigen presenting cells in each organs

Organ	Author	Disease	APC
Lung	Claire Mesnil[11]	Allergic sensitization	$CD11b^+$ DC
Intestine	Tordesillas,L[10]	Oral tolerance	$CD103^+$ DC
Brain	Derkow, K[13]	Encephalomyelitis	Plasmacytoid DC
Retina	Lehmann, U[14]	Retinal injury	$CD11b^+$ DC

APC, antigen presenting cell; DC, dendritic cell

Several studies have identified heterogeneous populations of corneal DCs,[8, 15-18] which play immunogenic roles in dry eye syndrome, corneal allotransplant, and autoimmune diseases,[18-23] or exhibit tolerogenic properties.[24] An imbalance in immunity contributes to the pathogenesis of dry eye diseases (DED).[25, 26] Given its worldwide prevalence, especially in elderly individuals,[27, 28] DED is a clinically relevant issue in today's society. Recently, the kinetics and functions of DCs have been investigated in ocular surface inflammation with DED.[29, 30]

The characteristics of DCs in the ocular surface or lacrimal glands (LGs) have been investigated intensively in experimental dry eye models.[20, 29, 31] However, a study on the DC distributions in the cornea or LG associated with an autoimmune model is currently under-investigated.

Therefore, we investigated whether dry eye syndrome in aged NOD.B10.H2^{b} mice (NOD mice), which mimic Sjögren's syndrome-like changes was due to aging or autoimmunity. [32-34] Aged C57BL/6 mice (B6) mice were used as the control group, and we conducted a study to find out which DC subsets are distinct in aged NOD mice.

2. Materials and Methods

2.1. Ethics declarations

The protocol was approved by the Institutional Animal Care and Use Committee of the Seoul National University Biomedical Research Institute (IACUC no. 20-0124-S1A1). Animal experiments were performed in accordance with the Association for Research in Vision and Ophthalmology (ARVO) statement for use of animals in ophthalmic vision and research and Animal Research: Reporting of In Vivo Experiments (ARRIVE) guidelines.

2.2. Animals

Eight C57BL/6 (B6) male mice and eight NOD.B10.H2^{b} male mice (The Jackson Laboratory, Bar Harbor, ME) were used in this study. Eight-week-old (n=4) and 20-month-old (n=4) B6 mice were included as the young and aged B6 group, while five-week- (n=4) and 24-week-old (n=4) NOD.B10.H2^{b} mice were included as the young and aged NOD group. The mice were bred in a specific pathogen-free facility at the Biomedical Research Institute of Seoul National University Hospital (Seoul, Korea), maintained at 22–24°C with 55±5% relative humidity, and provided free access to food and water.

2.3. Clinical evaluation of the dry eye

Corneal staining and tear secretion tests were performed under anesthesia (using a mixture of zoletil and xylazine at a ratio of 1:3). Corneal staining was blindly assigned by a single experienced ophthalmologist (Y. J.) using the National Eye Institute (NEI) scoring scheme. Fluorescein dye (0.25%) and Lissamine Green B (3%) (Sigma-Aldrich) were used for corneal staining in the B6 and NOD.B10.H2^{b} mice, respectively.[33, 35]

After placing one drop of dye on the conjunctival sac for 30 seconds, the ocular surface was gently washed with 1 mL of normal saline. Corneal staining was observed using a microscope (Olympus SZ61; Olympus Corporation, Tokyo, Japan). The B6 and NOD.B10.H2^{b} mice were observed using cobalt blue and white light (LED) illumination, respectively.[33, 35] For the tear secretion test, phenol red-impregnated cotton threads (FCI Ophthalmics, Pembroke, MA) were placed into the lateral canthus of mice for 60 seconds.

The old group weighed more than the young group (43.0±3.2 vs 22.7±0.5 in B6 mice, 31.3±0.8 vs 25.2±1.3 in NOD mice). To compensate for the difference in tear secretion volume induced by body weight, the tear secretion values were corrected with body weight according

to the method in the previous studiese.[36, 37]

2.4. Flow cytometry for analyzing immune cells

After the mice were euthanized, the cornea and limbal tissue (Co), extraorbital LG, and mesenteric lymph node (MLN) were extracted and collected. Bilateral tissues were pooled for analysis. To obtain a single-cell suspension, the tissues were treated with 1 mg/mL collagenase type I (Worthington, Lakewood, NJ) for 30 min at 37°C and homogenized through a 70-μm filter (BD BioSciences, San Diego, CA).

A single cell suspension was prepared by mincing the tissue between the frosted ends of two glass slides in RPMI-1640 medium (WelGENE, Daegu, Korea), 10% fetal bovine serum (FBS), and 1% penicillin-streptomycin. To sort dendritic cells (DCs), antigen-presenting MHC-II^{hi} B cells, macrophages, and granulocytes, including neutrophils and eosinophils, the cell populations were identified using the sequential gating strategy (Fig. 1). To exclude non-immune cells in Co and LG, the cells were gated with CD45 and the percentage of APC subsets was calculated in the $CD45^+$ parent population. The following antibodies were used for a subset: CD11b-PE-Cy7 (eBioscience, San Diego, CA), CD11c-PerCP-Cy5.5 (eBioscience), MHC-II-FITC (eBioscience), CD24-PE (eBioscience), and CD45-APC (eBioscience). To identify

82 $CD103^+$ dendritic cells (DC), CD103-PE (eBioscience) was applied to cells stained with
83 CD11b-PE-Cy7, CD11c-PerCP-Cy5.5, MHC-II-FITC, and CD45-APC in the other subset.
84 The stained cells were assayed using a FACSCanto flow cytometer (BD BioSciences, San Jose,
85 CA). Data were analyzed using FlowJo software (version 10.7.1) (Tree Star, Ashland, OR).
86 After forward-scatter and side-scatter gating, $CD45^+$ cells were gated (Fig. 1). The cells
87 were then further divided by CD11b and CD11c expression. Thereafter, each proportion was
88 sorted by the expression of CD24 and MHC-II or by the expression of CD103 and MHC-II
89 (Fig. 1). Antigens presenting MHC-II^{hi} B cells were identified with $CD45^+CD11b^-CD11c^-$
90 $CD24^+$MHC-II^{hi} (Fig. 1A).[38] Antigen-presenting MHC-II^{hi} macrophages (MHC-II^{hi} MQ) or
91 non-antigen-presenting macrophages were identified as $CD45^+CD11b^+CD11c^-CD24^-$MHC-
92 II^{hi} or $CD45^+CD11b^+CD11c^-CD24^-$MHC-$II^{lo}$ (Fig. 1B and C).[32] Within $CD11b^+$ cells,
93 neutrophils/eosinophils were isolated with $CD45^+CD11b^+CD11c^-CD24^+$MHC-$II^{lo}$ (Fig. 1D).[32]
94 Based on the expression of CD45, CD11c, CD24, and MHC-II as dendritic cells (DCs), DCs
95 were further divided into $CD11b^-$ DCs and $CD11b^+$ DCs (Fig. 1E and F).[32] $CD103^+CD11b^-$ DCs
96 and $CD103^+CD11b^+$ DCs were gated based on $CD45^+CD11b^-CD11c^+CD103^+$MHC-$II^{hi}$ and
97 $CD45^+CD11b^+CD11c^+CD103^+$MHC-$II^{hi}$ (Fig. 1G and H).[39]

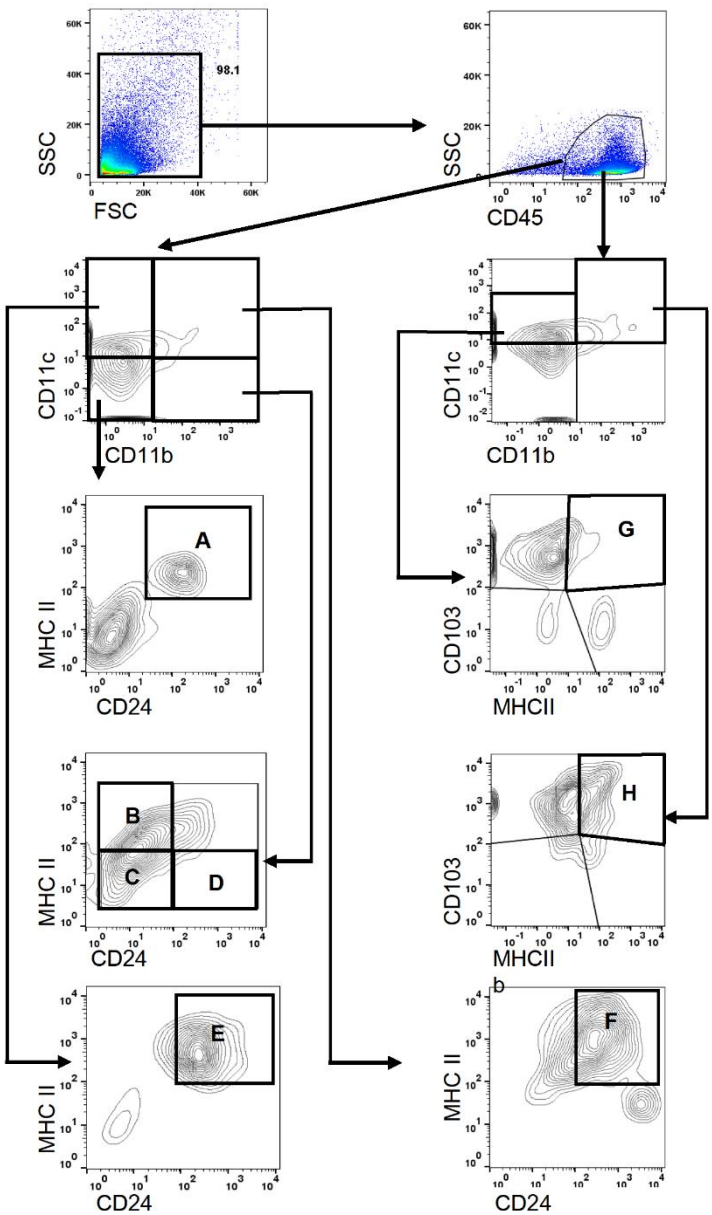
98.1
SSC
FSC
SSC
CD45
CD11c
CD11b
CD11c
CD11b
A
MHC II
CD24
G
CD103
MHCII
B
C
D
MHC II
CD24
H
CD103
MHCII
E
MHC II
CD24
F
MHC II
CD24

98

99

Figure 1. Gating strategy used to identify myeloid-cell and lymphoid-cell subsets. Following the exclusion of debris and cellular aggregates, forward-scatter and side-scatter gating were performed. The pan-hematopoietic marker CD45 was selected to distinguish immune cells from other corneal or lacrimal gland cells. A sequential gating strategy was used to identify populations expressing specific markers: (A) $CD45^{+}CD11b^{-}CD11c^{-}CD24^{+}MHC\text{-}II^{hi}$ cells as antigen-presenting $MHC\text{-}II^{hi}$ B cells, (B) $CD45^{+}CD11b^{+}CD11c^{-}CD24^{-}MHC\text{-}II^{hi}$ cells as antigen-presenting $MHC\text{-}II^{hi}$ macrophages ($MHC\text{-}II^{hi}$ MQ), (C) $CD45^{+}CD11b^{+}CD11c^{-}CD24^{-}MHC\text{-}II^{lo}$ cells as non-antigen-presenting macrophages ($MHC\text{-}II^{lo}$ MQ), (D) $CD11b^{+}CD11c^{-}CD24^{+}MHC\text{-}II^{lo}$ cells as neutrophils and eosinophils, (E) $CD11b^{-}CD11c^{+}CD24^{+}MHC\text{-}II^{hi}$ cells as $CD11b^{-}$ dendritic cells ($CD11b^{-}$ DC), (F) $CD11b^{+}CD11c^{+}CD24^{+}MHC\text{-}II^{hi}$ cells as $CD11b^{+}$ dendritic cells ($CD11b^{+}$ DC), (G) $CD45^{+}CD11b^{-}CD11c^{+}CD103^{+}MHC\text{-}II^{hi}$ cells as $CD103^{+}CD11b^{-}$ DC cells, and (H) $CD45^{+}CD11b^{+}CD11c^{+}CD103^{+}MHC\text{-}II^{hi}$ cells as $CD103^{+}CD11b^{+}$ DC cells.

2.5 16S Ribosomal RNA Analysis of fecal microbiota

Fecal pellets were directly collected from the anus of each mouse by holding it and allowing defecation. The collected feces were immediately stored at -80˚C until they were referred to Chunlab, Inc. (Seoul, Republic of Korea) for analysis. V3 to V4 region of 16S ribosomal RNA (rRNA) analysis was performed in the same way as described previously.[33, 40] Compositional differences, α- and β-diversities (using UniFrac), and linear discriminant analysis (LDA) effect size (LEfSe) were evaluated. Only those taxa that showed a *P*-value<0.05 and a log LDA score > 2 were ultimately considered for biomarker evaluation.[33]

2.6 Statistical Analyses

For comparing the two groups, independent t-test was used. Data are expressed as the mean ± standard error of the mean. Statistical analyses were performed using GraphPad Prism software (version 9.0; GraphPad Software, La Jolla, CA, USA). Differences were considered statistically significant at $P < 0.05$.

3. Results

Dry eye is manifest in aged B6 and NOD.B10.H2^b mice

In immunocompetent B6 mice, the average corneal stain scores of aged mice were significantly higher (13.63±1.51) than those of young mice (4.75±4.53) (P<0.001; Fig. 2A). Tear secretion was not significantly different between the groups (10.85±2.58 mm in young and 7.45±3.78 mm in aged mice) (P=0.054). However, when body weight (BW) was adjusted, the corrected value was significantly lower in aged mice (0.17±0.09/BW) than in young mice (0.48±0.12/BW) (P<0.001; Fig. 2B).

In autoimmune-susceptible NOD.B10.H2^b mice, the corneal stain scores of aged mice were significantly higher (10.50±2.14) than those of young mice (2.88±2.10) (P<0.001; Fig. 2C). A marked reduction in tear secretion was observed in aged mice. The tear secretion in young and aged mice was 4.86±0.47 mm and 3.44±0.35 mm, respectively (P<0.001). BW adjusted tear secretion was also significantly lower in the aged group (0.11±0.01/BW) than in the young group (0.19±0.03/BW) (P<0.001; Fig. 2D).

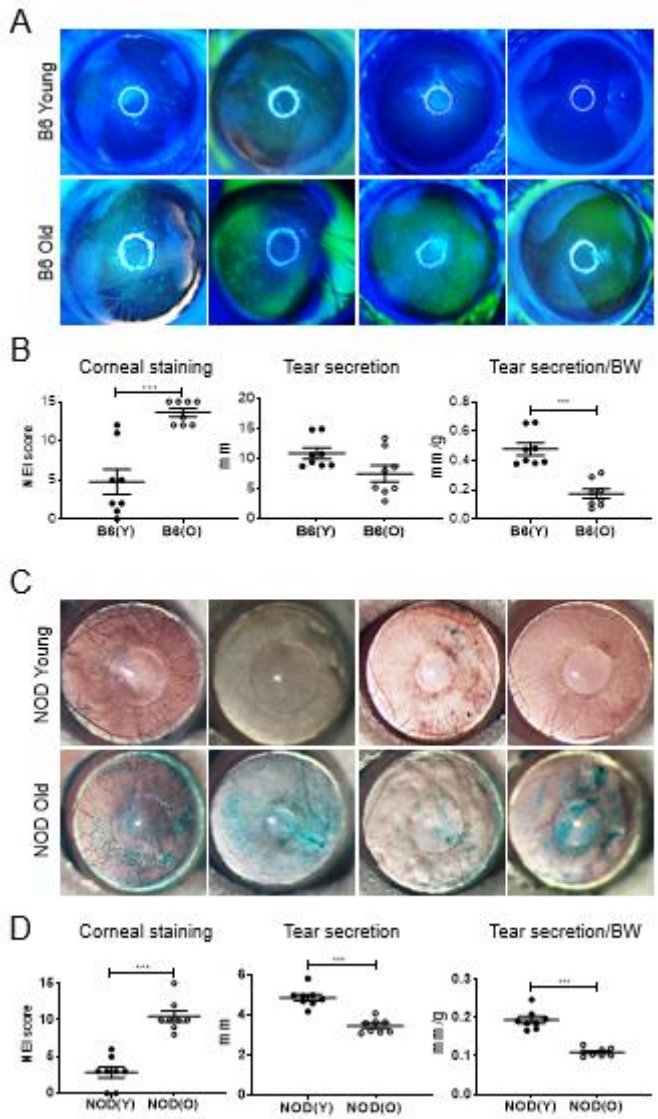
A
B6 Young
B6 Old
B
Corneal staining
Tear secretion
Tear secretion/BW
NEI score
mm
mm /g
B6(Y)
B6(O)
C
NOD Young
NOD Old
D
Corneal staining
Tear secretion
Tear secretion/BW
NEI score
mm
mm /g
NOD(Y)
NOD(O)

143

144

Figure 2. (A) Representative images of corneal fluorescein staining of young C57BL/6 (B6) mice (8-week-old; upper row) and aged B6 mice (20-month-old; lower low). (B) The National Eye Institute (NEI) corneal staining score was significantly higher in aged B6 mice than in young B6 mice ($P<0.001$). Body weight (BW) adjusted tear secretion was significantly lower in aged B6 mice than young B6 mice ($P<0.001$). (C) Representative images of corneal lissamine green staining of young NOD.B10.H2b mice (5-week-old; upper row) and aged NOD.B10.H2^b mice (24-week-old; lower row). (D) The NEI corneal staining score was significantly higher in aged NOD.B10.H2^b mice than in young NOD.B10.H2^b mice ($P<0.001$). Tear secretion and BW adjusted tear secretion were significantly lower in aged NOD.B10.H2^b mice than in young NOD.B10.H2^b mice ($P<0.001$). B6(Y), young B6 mice; B6(O), aged B6 mice; NOD(Y), young NOD.B10.H2^b mice; NOD(O), aged NOD.B10.H2^b mice. *$P<0.05$, **$P<0.01$, ***$P<0.001$

158 *Corneal CD11b^{+} DCs increased in aged mice*

159 In the cornea, the percentages of the CD45^{+} cell ratio showed no differences between the
160 young and aged groups in both of two models (P=0.580 and P=0.301, respectively) (Fig. 3). In
161 B6 mice, the percentage of corneal CD11b^{+} DCs (2.53±0.29%) was significantly higher in aged
162 mice than in young mice (1.43±0.38%) (P=0.004).

163 In NOD.B10.H2^{b} mice, the percentage of corneal CD11b^{+} DCs in aged mice was also
164 significantly higher (6.96±1.85%) than in young mice (0.54±0.48%) (P<0.001). By contrast,
165 the percentage of corneal CD11b^{-} DCs was lower in aged mice compared to young mice
166 (7.28±3.43% vs 17.73±5.45%) (P=0.019; Fig. 3B).

167

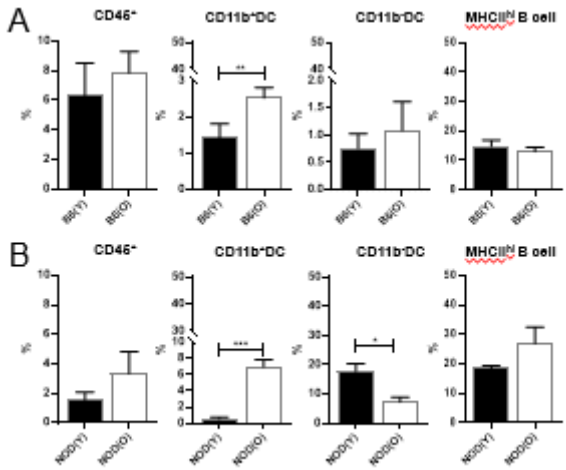

Figure 3. Corneal immune cell subsets in B6 (A) and NOD.B10.H2^{b} (B) mice. The total number of CD45^{+} cells was used as the denominator to compensate for the actual fraction of each subset. The percentage of CD11b^{+} DCs was higher in both aged B6 mice (A) (*P*=0.004) and aged NOD.B10.H2^{b} mice (B) (*P*<0.001) than in young mice, while the percentage of CD11b^{-} DCs was reduced in aged NOD.B10.H2^{b} mice (*P*=0.019). B6, C57BL/6; MHC, major histocompatibility complex; DC, dendritic cell; B6(Y), young B6 mice; B6(O), aged B6 mice; NOD(Y), young NOD.B10.H2^{b} mice; NOD(O), aged NOD.B10.H2^{b} mice. **P*<0.05, ***P*<0.01, ****P*<0.001.

Changes in MHC−II^{hi} B cells in LG of aged NOD.B10.H2^{b} mice

The percentages of the CD45^{+} cell ratio in the LG showed no differences between the young and aged groups (P=0.161 and P=0.297, respectively) (Fig. 4). In aged B6 mice, LG CD11b^{+} DCs were significantly lower (18.26±4.14%) than in young mice (25.28±3.65%) (P=0.044; Fig. 4A).

In the LG of NOD.B10.H2^{b} mice, no marked change in the DC subsets was observed. However, the percentage of MHC-II^{hi} B cells was significantly higher in aged NOD.B10.H2^{b} mice (7.84±2.52%) compared to young NOD.B10.H2^{b} mice (11.70±0.36%) (P=0.023; Fig. 4B).

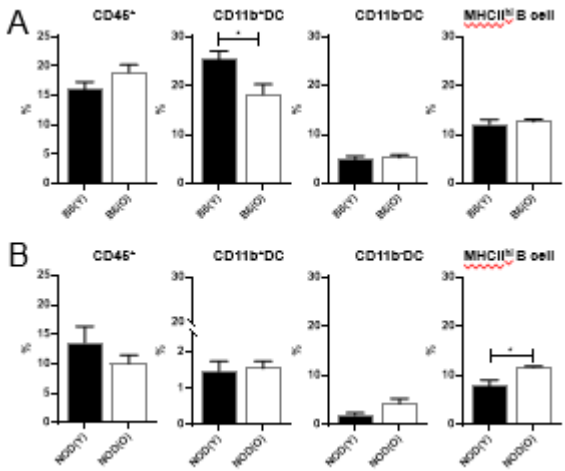

188

189 **Figure 4. Immune cell subsets of extraorbital lacrimal gland in B6 (A) and NOD. B10.H2^{b}**

190 **(B) mice.** The total number of CD45^{+} cells was used as the denominator to compensate for the actual

191 fraction of each subset. (A) The percentage of CD11b^{+} DC was significantly lower in aged B6 mice

192 (P=0.044). (B) The percentage of MHC-II^{hi} B cells was significantly higher in aged NOD.B10.H2^{b} mice

193 (P=0.023). B6, C57BL/6; MHC, major histocompatibility complex; DC, dendritic cell; B6(Y), young B6 mice;

194 B6(O), aged B6 mice; NOD(Y), young NOD.B10.H2^{b} mice; NOD(O), aged NOD.B10.H2b mice. *P<0.05,

195 **P<0.01, ***P<0.001.

196

Changes in APCs in MLN of aged mice

The percentage of $CD45^+$ cells in the MLN of aged mice did not increase compared to young mice ($P>0.05$; Fig. 5). The percentage of $CD11b^+$ DCs was significantly higher in aged B6 mice (4.27±1.07%) than in young B6 mice (2.82±0.09%) ($P=0.035$; Fig. 5A), which corresponded with the changes in the corneal $CD11b^+$ DCs. In NOD.B10.$H2^b$ mice, the percentage of MHC-II^{hi} B cells was significantly higher in the aged NOD.B10.$H2^b$ mice (1.96±0.42%) than in the young NOD.B10.$H2^b$ mice (1.30±0.26%) ($P=0.038$; Fig. 5B), which corresponded with the changes in MHC-II^{hi} B cells in the LG.

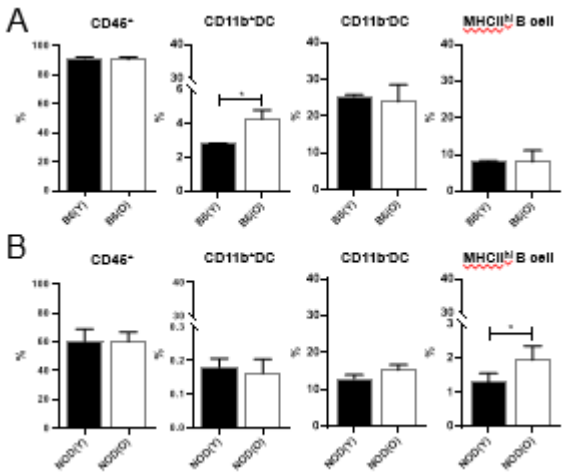

206

207 **Figure 5. Immune cell subsets of mesenteric lymph node in B6 (A) and NOD. B10.H2^{b}**

208 **(B) mice.** The percentage of CD45^{+} cells and the other subsets was calculated as the portion within total

209 cells. (A) The percentage of CD11b^{+} DC was significantly higher in aged B6 mice (P=0.035). (B) The

210 percentage of MHC-II^{hi} B cell was significantly higher in aged NOD.B10.H2^{b} mice (P=0.038). B6, C57BL/6;

211 MHC, major histocompatibility complex; DC, dendritic cell; B6(Y), young B6 mice; B6(O), aged B6 mice;

212 NOD(Y), young NOD.B10.H2^{b} mice; NOD(O), aged NOD.B10.H2^{b} mice. *P<0.05, **P<0.01, ***P<0.001.

213

Changes of corneal and nodal CD103$^+$ DC subsets in aged NOD.B10.H2^b mice

The percentages of $CD103^+CD11b^+$ DCs were significantly increased in the MLNs of both B6 and NOD.B10.H2^b mice ($P<0.05$; Fig. 6A and 6B). Notably, the percentages of nodal $CD103^+CD11b^-$DCs (1.29±0.17%) and $CD103^+CD11b^+$ DCs (0.32±0.07%) were significantly higher in aged NOD.B10.H2^b mice than in young mice (0.74±0.18%, P=0.004; vs. 0.11±0.05% P=0.002, respectively) (Fig. 6B). Correspondingly, the percentage of corneal $CD103^+CD11b^-$ DCs was markedly higher in aged mice (8.13±1.63%) than in young mice (0.25±0.29%) ($P<0.001$). However, in B6 mice, no differences were observed in terms of $CD103^+$ DCs in the cornea or LG (Fig. 6A), despite the increased frequency of nodal $CD103^+CD11b^+$DCs.

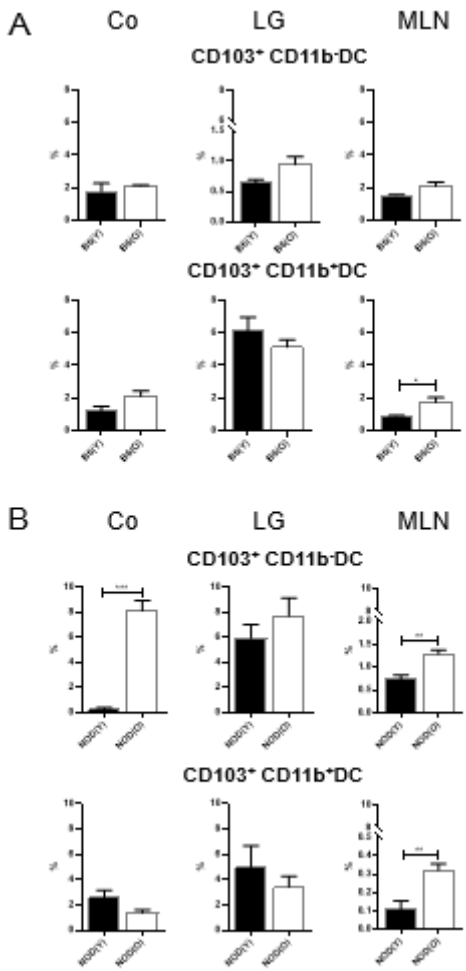
A
Co
LG
MLN
CD103+ CD11b-DC
CD103+ CD11b+DC
B
Co
LG
MLN
CD103+ CD11b-DC
CD103+ CD11b+DC

224

225

Figure 6. $CD103^+$ DC subsets of cornea (Co), lacrimal gland (LG), and mesenteric lymph node (MLN) in B6 (A) and NOD.B10.$H2^b$ (B) mice. In Co and LG, the percentage of subsets was calculated as the portion within $CD45^+$ cells. In MLN, the percentage of subsets was calculated as the percentage within total cells. (A) In MLN, the percentage of $CD103^+$ $CD11b^+$ DC was significantly higher in aged than young B6 mice (*P*=0.025), while the other subsets revealed no significant difference. (B) The percentage of $CD103^+CD11b^-$ DC was significantly higher in aged than young NOD.B10.$H2^b$ mice in Co (*P*<0.001). In MLN, the percentage of $CD103^+CD11b^-$ DC and $CD103^+CD11b^+$ DC was significantly higher in aged NOD.B10.$H2^b$ mice (*P*=0.004 and *P*=0.002, respectively). B6, C57BL/6; MHC, major histocompatibility complex; DC, dendritic cell; B6(Y), young B6 mice; B6(O), aged B6 mice; NOD(Y), young NOD.B10.$H2^b$ mice; NOD(O), aged NOD.B10.$H2^b$ mice. **P*<0.05, ***P*<0.01, ****P*<0.001.

No proportional changes of corneal macrophages/granulocytes in aged mice

No significant proportional changes were observed in the MHC-II^{hi} MQ or neutrophils/eosinophils ($CD45^{+}CD11b^{+}CD11c^{-}CD24^{+}MHC^{lo}$) in the cornea of both B6 and NOD.B10.H2^{b} mice (Fig. 7). In both mice, the percentage of MHC-II^{hi} MQ of LG was lower in the aged group than in the young group (P<0.05) (Fig. 7). The percentage of neutrophils/eosinophils of LG was also lower in aged NOD.B10.H2^{b} mice than in young mice (P=0.022) (Fig. 7). In contrast, MLN showed a considerably increased proportion of MHC-II^{hi} MQ in NOD.B10.H2^{b} mice and the proportion of neutrophils/eosinophils in both aged mice. However, this was clinically negligible due to the very low proportion (P<0.05) (Fig. 7).

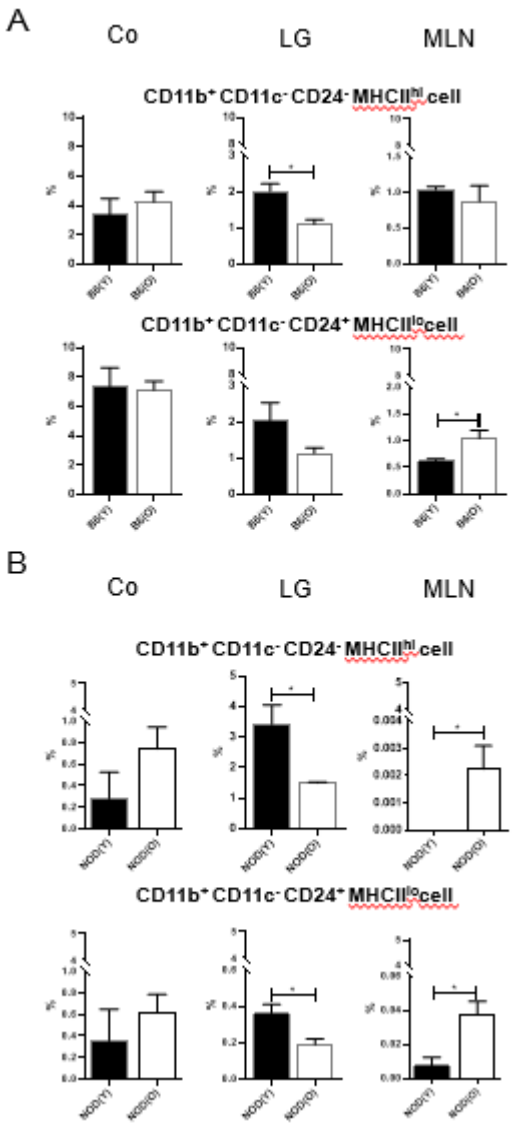
A
Co
LG
MLN
CD11b+CD11c-CD24-MHCIIhi cell
CD11b+CD11c-CD24+MHCIIlo cell
B
Co
LG
MLN
CD11b+CD11c-CD24-MHCIIhi cell
CD11b+CD11c-CD24+MHCIIlo cell

248

249

250

Figure 7. MHC-II^{hi} MQ (CD11b^{+}CD11c^{-}CD24^{-}MHC-II^{hi}) and neutrophils/eosinophils (CD45^{+}CD11b^{+}CD11c^{-}CD24^{+}MHC-II^{lo}) in cornea (Co), lacrimal gland (LG), and mesenteric lymph node (MLN) in B6 (A) and NOD.B10.H2^{b} (B) mice. In Co and LG, the percentage of subsets was calculated as the portion within CD45^{+} cells. In MLN, the percentage of subsets was calculated as the portion within total cells. (A) The percentage of MHC-II^{hi} MQ was significantly lower in aged than young B6 mice in LG (P=0.010). The percentage of neutrophils/eosinophils was significantly higher in aged B6 mice than young B6 mice in MLN (P=0.032). (B) The percentage of MHC-II^{hi} MQ and neutrophils/eosinophils in LG was significantly lower in aged than in young NOD.B10.H2^{b} mice (P=0.024 and P=0.022, respectively). However, the percentage of MHC-II^{hi} MQ and neutrophil/eosinophil in MLN was significantly higher in aged NOD.B10.H2^{b} mice (P=0.039 and P=0.015, respectively). MQ, Macrophage; B6, C57BL/6; B6(Y), young B6 mice; B6(O), aged B6 mice; MHC, major histocompatibility complex; NOD(Y), young NOD.B10.H2^{b} mice; NOD(O), aged NOD.B10.H2^{b} mice. *P<0.05, **P<0.01, ***P<0.001.

Aging-dependent compositional changes of intestinal microbiome in B6 mice

For α-diversity analysis, the number of operational taxonomic units (OTU), Chao1 index (indicating species richness), and Shannon diversity index were used. The Shannon index was significantly higher in aged B6 mice (P=0.029; Mann Whitney U test) (Fig. 8A); however, the number of OTU and Chao1 index did not differ between groups. The β-diversity of the genus and species analyzed by UniFrac principal coordinates analysis revealed a significant distance between the young and aged B6 groups (P=0.036; permutational multivariate analysis of variance) (Fig. 8B).

Linear discriminant analysis effect size (LEfSe) exhibited significant biological taxonomic differences between groups (Fig. 8C). Nine microbial taxa in the aged B6 group, such as *Lachnospiraceae* (family), *Helicobacteraceae* (family), and *Muribaculum* (genus), were higher in abundance than in the young B6 group, whereas eight microbial taxa in the young B6 group, such as *Lactobacillaceae* (family), *Prevotella* (genus), *Lactobacillus intestinalis* (species), *Lactobacillus reuteri* (species), and *Lactobacillus gasseri* (species), were higher in abundance compared to the aged B6 group.

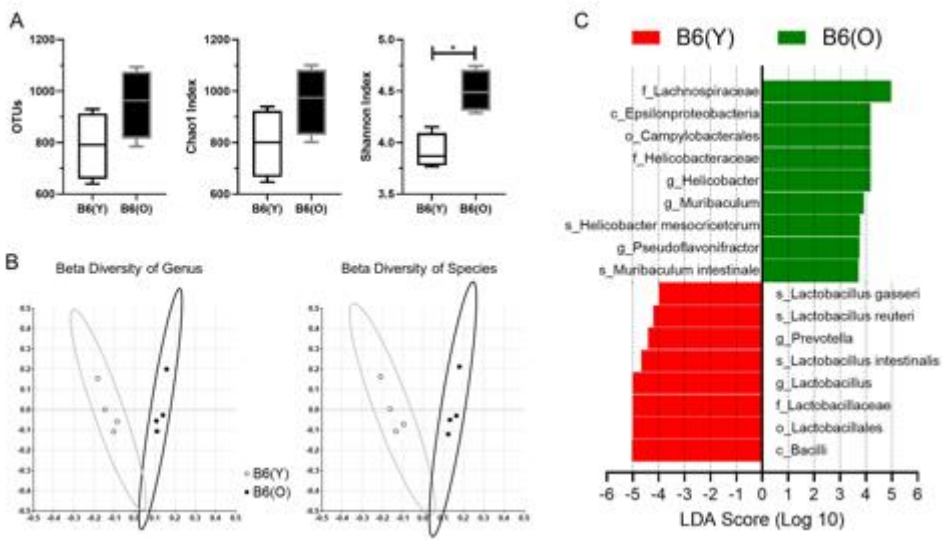

282

283 **Figure 8. Microbiome analysis in B6 mice age-related dry eye model.** (A) Results of α-
284 diversity analysis. Observed operational taxonomic unit (OTU) count, Chao1 index (indicating species
285 richness), and Shannon diversity index were used. Shannon index was significantly higher in aged B6 mice
286 (*P*=0.029; Mann Whitney U test). (B) β-diversity of genus and species analyzed by UniFrac principal
287 coordinates analysis indicated significant distances between young and aged B6 mice (*P*=0.036;
288 permutational multivariate analysis of variance). (C) Linear discriminant analysis (LDA) effect size (LEfSe)
289 performed on the microbial community with cut-off LDA score >2.0. B6, C57BL/6; B6(Y), young B6 mice;
290 B6(O), aged B6 mice. Bars indicate maximum and minimum values.

291

292

4. Discussion

To the best of our knowledge, this is the first descriptive study of age-dependent APC changes in both immunocompetent and immunosusceptible mice. This study indicates that APCs involved in aging-dependent dry eye and autoimmune dry eye are different and gut-related $CD103^+CD11b^-$DCs and $MHC\text{-}II^{hi}$ B cells may be the prevailing APCs in the ocular surface–LG axis of aged NOD.B10.$H2^b$ mice. However, corneal $CD11b^+$ DCs tended to increase in aged B6 mice.

We focused on the changes in three subsets of DCs, namely $CD11b^+$ DCs, $CD11b^-$ DCs, and $CD103^+$ DCs.[8, 41] $CD103^+$ DCs act in self or foreign antigen recognition or in the induction of gut-related molecules on effector T cells.[41] Interferon (IFN) -α-producing plasmacytoid DCs are pathogenic cells that enhance pro-inflammatory cytokine production in Sjögren's syndrome.[42, 43] $CD11c^+CD86^+$ and $CD11b^+CD11c^-$ cells are involved in experimental dry eye models.[20, 29] B cells detect and initiate their immune responses to antigens and present antigens to T cells.[44-46] Given that B cells are crucial for the pathogenesis of Sjögren's syndrome,[47] DCs or antigen-presenting B cells may be responsible for aggravating the inflammatory responses in

either aged B6 or autoimmune Sjögren's syndrome-like mice.

Heterogeneous groups of APCs exist in the cornea and [23,48] have been investigated for their role in different inflammatory corneal diseases.[49-52] In this study, $CD11b^+$ DCs were found to increase on the ocular surface in both aged B6 and autoimmune Sjögren's syndrome-like mice. Among the APCs, conventional dendritic cells (cDCs) that express high levels of CD11c and MHC-II and low levels of F4/80 exhibited a superior capacity to present antigens to T cells.[53] cDC can be further sub-classified into type 1 cDC (cDC1) and type 2 cDC (cDC2).[53] The former induces cytotoxic $CD8^+$ T cell and T helper1 (Th1) responses, while the latter initiates Th2, Th17, and T regulatory (Treg) responses.[53] cDC1 can be identified as $CD4^-CD8\alpha^+CD11b^-$ and cDC2 can be identified as $CD4^+CD8\alpha^-CD11b^+$. In gut nonlymphoid tissues, cDC1s are classified as $CD103^+CD11b^-CD11c^+MHC\text{-}II^{hi}$, whereas cDC2s comprise both $CD103^+CD11b^+CD11c^+MHC\text{-}II^{hi}$ and $CD103^-CD11b^+CD11c^+MHC\text{-}II^{hi}$.[53] Surprisingly, $CD103^+CD11b^-$DCs are remarkably increased in both the cornea and MLN in aged NOD.B10.$H2^b$ mice, suggesting an increase in the number of presumed $CD103^+$ conventional DC1s. $CD45^+CD11b^-CD11c^+CD24^+MHC\text{-}II^{hi}$ cells or $CD45^+CD11b^+CD11c^+CD24^+MHC\text{-}II^{hi}$ cells are considered cDC1 ($CD11b^+$ DC) or cDC2 ($CD11b^-$ DC). However, further detailed identification is needed using additional markers, such as CD8α and CD4. Nevertheless, this

outcome provides an insight into how the distribution of $CD11b^{+/-}$ DCs or $CD103^{+}$ DCs changes in the cornea and LG depending on age and autoimmunity. In the present study, the mechanisms underlying the changes in the matured status of each type of APC were not evaluated. Given that the different distributions and maturity of APCs may have an effect on triggering immune responses, the different status of matured DCs should be investigated further using additional markers, namely CD86 or CD80.

Recent evidence indicates that both B and T cells play a major role in the pathogenesis of Sjögren's syndrome.[54] NOD.B10-$H2^{b}$ mice exhibit many features of Sjögren's syndrome, including exocrine gland dysfunction concomitant with leukocyte infiltration of the salivary and LGs.[55] Recent studies have shown that both Sjögren's syndrome patients and NOD.B10-$H2^{b}$ mice exhibit increased B lymphocyte survival, B cell hyper-reactivity, and hyper-gammaglobulinemia with a high production of autoantibodies.[55] In our study, antigen-presenting MHC-II^{hi} B cells tended to increase in both LG and MLN with aging in NOD.B10-$H2^{b}$ mice, suggesting that B cells may be an important factor, not only as an effector cell to produce antibodies, but also as an APC in autoimmune Sjögren's syndrome-like dry eye. On the other hand, no changes in MHC-II^{hi} B cells were observed in aged B6 mice, indicating that

antigen-presenting B cells may not to be involved in the pathogenesis of immune competent dry eye. This change in the APCs in the LG is distinct from the change in corneal APC, suggesting that heterogeneous aging-dependent distributions of APC vary depending on the tissues. Given that gut dysbiosis has a significant impact on the maturation and differentiation of B cells.[56] An increase in mesenteric nodal MHC-II^{hi} B cells may be gut-related. Considering that recent studies have shown that intestinal dysbiosis is related to autoimmune dry eyes.[33, 57, 58] the increase in LG MHC-II^{hi} B cells observed in the present study may correspond to changes in the gut. In primary Sjögren's syndrome, CD27^{+} memory B cells, marginal zone B cells, plasmablasts, and plasma cells are the key subsets of B cells.[47] To acknowledge the functional changes of effector B cells, further investigation should be performed using CD19, CD20, and CD38, or measured using antibodies.[59]

Regarding the results of the intestinal microbiome, we found that the diversity of the intestinal microbiome increased in aged B6 mice. Microbiome composition was significantly different between the aged and young B6 mice, which was clearly observed in the principal coordinates analysis plot (Fig. 8B). Emerging evidence implies that the intestinal microbiome contributes to DC maturation and differentiation by modulating the intestinal epithelial barrier,

361 inhibiting pathogens, regulating systemic immune response, or secreting probiotic-derived
362 factors.[60-63]

363 In this study, aged B6 mice showed decreased family *Lactobacillaceae*, including
364 *Lactobacillus reuteri* and *Lactobacillus gasseri*, and increased family *Lachnospiraceae* and
365 *Helicobacteraceae*. Many species of *Lactobacillus* (probiotics) exert immunomodulatory
366 functions *in vitro* and *in vivo*.[62] *Lactobacilli* strains facilitate the production of short-chain fatty
367 acids and induce tolerogenic DCs, which promote naïve $CD4^+$ T cells into Tregs.[64] The oral
368 administration of *Lactobacillus gasseri* reduced $CD11c^+CD103^+$ cells in the lamina propria and
369 enhanced oral tolerance by increasing regulator T cells.[65, 66] *Lactobacillus gasseri*
370 downregulated the production of interleukin-12 and tumor necrosis factor-α in mature DCs *in*
371 *vitro*.[66] In contrast, family *Lachnospiraceae* was increased in diabetic mice, and negatively
372 correlated with splenic $CD11b^+CD11c^+$ tolerogenic DC and Treg.[67] Family *Helicobacteraceae*
373 belongs to phylum *Proteobacteria*, and is considered a microbial signature of intestinal
374 dysbiosis. Family *Helicobacteraceae* increased in an acute colitis mouse model that showed
375 lower $CD11c^+CD103^+$ tolerogenic DCs in the lamina propria, which decreased as colitis
376 improved.[9] In this study, $CD11b^+$ DCs were increased in both the cornea and MLN of aged B6
377 mice. However, the direct association between the intestinal microbiome and DC subsets could

not be analyzed because of the small sample size. Nevertheless, age-related intestinal dysbiosis seems to affect the DC subsets, which is distinct from the age-dependent changes of DC subsets in NOD.B10.H2^{b} mice. In previous studies, abnormal composition of microbiome in autism and cancer was reported, and it was confirmed that the symptoms and treatment outcomes were improved through microbiota transplantation.[68, 69] In our study, young group and old group showed a marked difference in microbiome composition, and further investigation is needed to confirm that dry eye syndrome is improved through fecal microbiome transplantation.

This study has several limitations. First, only male mice were used because female NOD.B10.H2^{b} mice tend to develop only sialadenitis instead of dacryoadenitis.[70] Only B6 male mice were included to match the sex with NOD.B10.H2^{b} mice. However, the female sex is one of the highest risk factors for dry eye syndrome, due to the effects of hormones on this disorder.[71] Therefore, it is not possible to apply female-associated dry eye. Second, because only a small number of animals was used, the results may not be statistically representative of each group. Third, a flow cytometry machine capable of sorting up to five channels were used. Therefore, the use of additional specific markers to differentiate between neutrophil and eosinophil, cDC1 and cDC2, or mature DC and immature DCs was not possible.[40] Lastly, only the changes in the

gut microbiome related to aging were analyzed, and no cause-and-effect relationship was observed. Further studies are needed to determine whether there are changes in the dendritic cells and the gut microbiome after treatment of dry eye.

In conclusion, the results demonstrate that there is a distinct heterogeneous distribution of DCs in corneal and LG tissue between immunocompetent and autoimmune aging-related dry eye models. An increase in corneal $CD103^{+}CD11b^{-}$ DCs and LG MHC-II^{hi} B cells may be accompanied by an increase in nodal $CD103^{+}CD11b^{-}$ DCs and MHC-II^{hi} B cells in aging-dependent Sjögren's syndrome-like mice, whereas no differences of $CD103^{+}$ DCs are observed in aging-related dry eye.

References

1. Steinman RM, Cohn ZA. Identification of a novel cell type in peripheral lymphoid organs of mice. I. Morphology, quantitation, tissue distribution. J Exp Med 1973;137:1142-1162.

2. Banchereau J, Steinman RM. Dendritic cells and the control of immunity. Nature 1998;392:245-252.

3. Steinman RM. Lasker Basic Medical Research Award. Dendritic cells: versatile controllers of the immune system. Nat Med 2007;13:1155-1159.

4. Sojka DK, Huang YH, Fowell DJ. Mechanisms of regulatory T-cell suppression - a diverse arsenal for a moving target. Immunology 2008;124:13-22.

5. Hasegawa H, Matsumoto T. Mechanisms of Tolerance Induction by Dendritic Cells In Vivo. Front Immunol 2018;9:350.

6. Cifuentes-Rius A, Desai A, Yuen D, Johnston APR, Voelcker NH. Inducing immune tolerance with dendritic cell-targeting nanomedicines. Nat Nanotechnol 2020.

7. Agrawal A, Gupta S. Impact of aging on dendritic cell functions in humans. Ageing Res Rev 2011;10:336-345.

8. Forrester JV, Xu H, Kuffová L, Dick AD, McMenamin PG. Dendritic cell physiology and function in the eye. Immunol Rev 2010;234:282-304.

9. Chinnery HR, Humphries T, Clare A, et al. Turnover of bone marrow-derived cells in the irradiated mouse cornea. Immunology 2008;125:541-548.

10. Hamrah P, Liu Y, Zhang Q, Dana MR. Alterations in corneal stromal dendritic cell phenotype

and distribution in inflammation. Arch Ophthalmol 2003;121:1132-1140.

11. Liu Y, Hamrah P, Zhang Q, Taylor AW, Dana MR. Draining lymph nodes of corneal transplant hosts exhibit evidence for donor major histocompatibility complex (MHC) class II-positive dendritic cells derived from MHC class II-negative grafts. J Exp Med 2002;195:259-268.

12. Hamrah P, Liu Y, Zhang Q, Dana MR. The corneal stroma is endowed with a significant number of resident dendritic cells. Invest Ophthalmol Vis Sci 2003;44:581-589.

13. Schonberg A, Hamdorf M, Bock F. Immunomodulatory Strategies Targeting Dendritic Cells to Improve Corneal Graft Survival. J Clin Med 2020;9.

14. Maruoka S, Inaba M, Ogata N. Activation of Dendritic Cells in Dry Eye Mouse Model. Invest Ophthalmol Vis Sci 2018;59:3269-3277.

15. Vogelsang P, Jonsson MV, Dalvin ST, Appel S. Role of dendritic cells in Sjögren's syndrome. Scand J Immunol 2006;64:219-226.

16. Hamrah P, Zhang Q, Liu Y, Dana MR. Novel characterization of MHC class II-negative population of resident corneal Langerhans cell-type dendritic cells. Invest Ophthalmol Vis Sci 2002;43:639-646.

17. Dana MR. Corneal antigen-presenting cells: diversity, plasticity, and disguise: the Cogan lecture. Invest Ophthalmol Vis Sci 2004;45:722-727; 721.

18. Egan RM, Yorkey C, Black R, et al. In vivo behavior of peptide-specific T cells during mucosal tolerance induction: antigen introduced through the mucosa of the conjunctiva elicits prolonged antigen-specific T cell priming followed by anergy. J Immunol 2000;164:4543-4550.

19. Luo L, Li DQ, Doshi A, Farley W, Corrales RM, Pflugfelder SC. Experimental dry eye

446 stimulates production of inflammatory cytokines and MMP-9 and activates MAPK signaling pathways
447 on the ocular surface. Invest Ophthalmol Vis Sci 2004;45:4293-4301.
448 20. Stern ME, Gao J, Schwalb TA, et al. Conjunctival T-cell subpopulations in Sjögren's and non-
449 Sjögren's patients with dry eye. Invest Ophthalmol Vis Sci 2002;43:2609-2614.
450 21. Paulsen AJ, Cruickshanks KJ, Fischer ME, et al. Dry eye in the beaver dam offspring study:
451 prevalence, risk factors, and health-related quality of life. Am J Ophthalmol 2014;157:799-806.
452 22. de Paiva CS. Effects of Aging in Dry Eye. Int Ophthalmol Clin 2017;57:47-64.
453 23. Lee HS, Amouzegar A, Dana R. Kinetics of Corneal Antigen Presenting Cells in Experimental
454 Dry Eye Disease. BMJ Open Ophthalmol 2017;1:e000078.
455 24. Perez VL, Stern ME, Pflugfelder SC. Inflammatory basis for dry eye disease flares. Exp Eye
456 Res 2020;108294.
457 25. Ortiz G, Chao C, Jamali A, et al. Effect of Dry Eye Disease on the Kinetics of Lacrimal Gland
458 Dendritic Cells as Visualized by Intravital Multi-Photon Microscopy. Front Immunol 2020;11:1713.
459 26. Misharin AV, Morales-Nebreda L, Mutlu GM, Budinger GR, Perlman H. Flow cytometric
460 analysis of macrophages and dendritic cell subsets in the mouse lung. Am J Respir Cell Mol Biol
461 2013;49:503-510.
462 27. Choi SH, Oh JW, Ryu JS, et al. IRT5 Probiotics Changes Immune Modulatory Protein
463 Expression in the Extraorbital Lacrimal Glands of an Autoimmune Dry Eye Mouse Model. Invest
464 Ophthalmol Vis Sci 2020;61:42.
465 28. Lee H, Kim CE, Ahn BN, Yang J. Anti-inflammatory effect of hydroxyproline-
466 GQDGLAGPK in desiccation stress-induced experimental dry eye mouse. Sci Rep 2017;7:7413.

29. Moon J, Ryu JS, Kim JY, Im SH, Kim MK. Effect of IRT5 probiotics on dry eye in the experimental dry eye mouse model. PLoS One 2020;15:e0243176.

30. Yuan Y, Zhou J, Zheng Y, et al. Beneficial effects of polysaccharide-rich extracts from Apocynum venetum leaves on hypoglycemic and gut microbiota in type 2 diabetic mice. Biomed Pharmacother 2020;127:110182.

31. Merad M, Sathe P, Helft J, Miller J, Mortha A. The dendritic cell lineage: ontogeny and function of dendritic cells and their subsets in the steady state and the inflamed setting. Annu Rev Immunol 2013;31:563-604.

32. Daley JM, Thomay AA, Connolly MD, Reichner JS, Albina JE. Use of Ly6G-specific monoclonal antibody to deplete neutrophils in mice. J Leukoc Biol 2008;83:64-70.

33. del Rio ML, Bernhardt G, Rodriguez-Barbosa JI, Forster R. Development and functional specialization of CD103+ dendritic cells. Immunol Rev 2010;234:268-281.

34. Hillen MR, Pandit A, Blokland SLM, et al. Plasmacytoid DCs From Patients With Sjögren's Syndrome Are Transcriptionally Primed for Enhanced Pro-inflammatory Cytokine Production. Front Immunol 2019;10:2096.

35. Gottenberg JE, Cagnard N, Lucchesi C, et al. Activation of IFN pathways and plasmacytoid dendritic cell recruitment in target organs of primary Sjögren's syndrome. Proc Natl Acad Sci U S A 2006;103:2770-2775.

36. Alonso-Ramirez R, Loisel S, Buors C, et al. Rationale for Targeting CD6 as a Treatment for Autoimmune Diseases. Arthritis 2010;2010:130646.

37. Rock KL, Benacerraf B, Abbas AK. Antigen presentation by hapten-specific B lymphocytes.

I. Role of surface immunoglobulin receptors. J Exp Med 1984;160:1102-1113.

38. Batista FD, Harwood NE. The who, how and where of antigen presentation to B cells. Nature Reviews Immunology 2009;9:15-27.

39. Nocturne G, Mariette X. B cells in the pathogenesis of primary Sjogren syndrome. Nat Rev Rheumatol 2018;14:133-145.

40. Hamrah P, Dana MR. Corneal antigen-presenting cells. Chem Immunol Allergy 2007;92:58-70.

41. Saban DR. The chemokine receptor CCR7 expressed by dendritic cells: a key player in corneal and ocular surface inflammation. Ocul Surf 2014;12:87-99.

42. Jamali A, Hu K, Sendra VG, et al. Characterization of Resident Corneal Plasmacytoid Dendritic Cells and Their Pivotal Role in Herpes Simplex Keratitis. Cell Rep 2020;32:108099.

43. Jamali A, Kenyon B, Ortiz G, et al. Plasmacytoid dendritic cells in the eye. Prog Retin Eye Res 2020;100877.

44. Jamali A, Seyed-Razavi Y, Chao C, et al. Intravital Multiphoton Microscopy of the Ocular Surface: Alterations in Conventional Dendritic Cell Morphology and Kinetics in Dry Eye Disease. Front Immunol 2020;11:742.

45. Sun T, Nguyen A, Gommerman JL. Dendritic Cell Subsets in Intestinal Immunity and Inflammation. J Immunol 2020;204:1075-1083.

46. Tobon GJ, Pers JO, Youinou P, Saraux A. B cell-targeted therapies in Sjogren's syndrome. Autoimmun Rev 2010;9:224-228.

47. Nguyen C, Cornelius J, Singson E, Killedar S, Cha S, Peck AB. Role of complement and B

lymphocytes in Sjogren's syndrome-like autoimmune exocrinopathy of NOD.B10-H2b mice. Mol Immunol 2006;43:1332-1339.

48. Zhao Q, Elson CO. Adaptive immune education by gut microbiota antigens. Immunology 2018;154:28-37.

49. Moon J, Choi SH, Yoon CH, Kim MK. Gut dysbiosis is prevailing in Sjögren's syndrome and is related to dry eye severity. PLoS One 2020;15:e0229029.

50. Moon J, Yoon CH, Choi SH, Kim MK. Can Gut Microbiota Affect Dry Eye Syndrome? Int J Mol Sci 2020;21.

51. Sundling C, Ronnberg C, Yman V, et al. B cell profiling in malaria reveals expansion and remodelling of CD11c+ B cell subsets. JCI Insight 2019;5.

52. Weiss G, Christensen HR, Zeuthen LH, Vogensen FK, Jakobsen M, Frøkiær H. Lactobacilli and bifidobacteria induce differential interferon-β profiles in dendritic cells. Cytokine 2011;56:520-530.

53. Mazzeo MF, Luongo D, Sashihara T, Rossi M, Siciliano RA. Secretome Analysis of Mouse Dendritic Cells Interacting with a Probiotic Strain of Lactobacillus gasseri. Nutrients 2020;12.

54. Christensen HR, Frøkiaer H, Pestka JJ. Lactobacilli differentially modulate expression of cytokines and maturation surface markers in murine dendritic cells. J Immunol 2002;168:171-178.

55. Mangalam A, Shahi SK, Luckey D, et al. Human Gut-Derived Commensal Bacteria Suppress CNS Inflammatory and Demyelinating Disease. Cell Rep 2017;20:1269-1277.

56. Liu Y, Alookaran JJ, Rhoads JM. Probiotics in Autoimmune and Inflammatory Disorders. Nutrients 2018;10.

57. Aoki-Yoshida A, Yamada K, Hachimura S, et al. Enhancement of Oral Tolerance Induction in

530 DO11.10 Mice by Lactobacillus gasseri OLL2809 via Increase of Effector Regulatory T Cells. PLoS One
531 2016;11:e0158643.
532 58. Luongo D, Miyamoto J, Bergamo P, et al. Differential modulation of innate immunity in vitro
533 by probiotic strains of Lactobacillus gasseri. BMC Microbiol 2013;13:298.
534 59. Krych Ł, Nielsen DS, Hansen AK, Hansen CH. Gut microbial markers are associated with
535 diabetes onset, regulatory imbalance, and IFN-γ level in NOD mice. Gut Microbes 2015;6:101-109.
536 60. Ooi JH, Li Y, Rogers CJ, Cantorna MT. Vitamin D regulates the gut microbiome and protects
537 mice from dextran sodium sulfate-induced colitis. J Nutr 2013;143:1679-1686.
538 61. Doyle ME, Boggs L, Attia R, et al. Autoimmune dacryoadenitis of NOD/LtJ mice and its
539 subsequent effects on tear protein composition. Am J Pathol 2007;171:1224-1236.
540 62. Sullivan DA, Rocha EM, Aragona P, et al. TFOS DEWS II Sex, Gender, and Hormones
541 Report. Ocul Surf 2017;15:284-333.
542

초록

자가면역성 건성안 쥐모델에서의

$CD103^+$ 수지상 세포의 분포 변화

서울대학교 대학원 의학과

안과학 전공

정영호

목적: 우리는 노화 및 자가면역성 건성안 쥐 모델에서의 특징적인 항원표지세포의 분포에 대해서 연구하고자 이번 연구를 계획 하였다.

방법: 노화 관련 건성안 쥐모델로 C57BL/6 (B6) 쥐를 선정하였고, 8주령 쥐를 어린 쥐, 20개월령을 나이든 쥐로 설정 하였다. 자가면역성 건성안 쥐 모델로 NOD.B10.$H2^b$ 쥐를 사용 하였고, 5주령을 어린 쥐, 24 주령을 나이든 쥐로 정하였다. 각 군은 각막 염색 점수, 눈물분비량을 측정 및 비교 하였고, 각막, 눈물샘, 장간막 림프절의 항원표지세포도 유세포 분석기를 통하여 분석하였다. 또한 B6 쥐의 분변을 모아서 장내 마이크로바이옴의 구성도 비교 분석 하였다.

559 **결과:** 모든 군에서 나이든 쥐가 건성안 양상이 심해지는 것이 관찰되었다. B6
560 쥐의 수지상 세포 분석에서 각막 $CD11b^+$ 수지상 세포가 나이든 쥐에서
561 유의하게 증가하였고 ($P<0.05$), 장간막 $CD11b^+$ 수지상세포와 $CD103^+CD11b^+$
562 수지상세포가 유의하게 증가하였다 ($P<0.05$).
563 NOD 쥐에서는 각막의 $CD103^+CD11b^-$ 수지상세포와 눈물샘의
564 $MHC-II^{hi}$ B 세포가 노화에 따라 유의 하게 증가하였다. 장간막
565 $CD103^+CD11b^+$ 수지상세포, $CD103^+CD11b^-$ 수지상세포와 $MHC-II^{hi}$ B
566 세포도 유의하게 노화에 따라 증가한 양상을 보였다. B6 쥐의 장내
567 마이크로바이옴 구성 분석에서, beta-diversity 분석에서 genus 와 species
568 분석 시 양군간의 유의한 차이를 확인할 수 있었다. 대표적으로 나이든 쥐에서
569 *Lachnospiraceae* 와 *Helicobacteraceae* 를 포함한 9개의 균주가 더 많이 분포했고,
570 어린 쥐에서는 *Lactobacillus* 를 포함한 8개의 균주가 더 많이 분포 하였다.
571
572 **결론:** 장 관련 $CD103^+CD11b^-$수지상세포 및 $MHC-II^{hi}$ B 세포는 자가 면역

573 건성안 모델에서 많은 분포를 확인 하였지만, $CD103^+$ DC의 경우 노화 관련

574 건성안에서는 특징적인 분포를 확인 할 수 없었다.

575

576 **주요어** : 자가면역질환, 수지상 세포, 항원 표지세포, CD103 수지상세포,

577 $MHC-II^{hi}$

578

579 **학 번** : 2016-21948

580

감사의 글

2020년 봄에 군의관 복무를 마치면서, 군휴학 복학 서류를 낼때가 생각이 납니다. 군의관때 안과 진료를 볼 수 없는 환경에서 근무를 일부 했던 터라, 다시 대학병원에 돌아간다는 것에 막연한 두려움이 있었고, 동물실험 및 면역학에 대한 지식이 전무 하였기에 이번 연구를 시작 함에 있어서 과연 해낼 수 있을까 스스로도 의문이었습니다.

처음 실험 설계를 위한 회의를 가지었을 때, 수지상 세포와 항원 표지세포에 이전의 연구들을 배우고, 수지상 세포의 역할에 대한 기존의 연구 논문을 읽으면서도 그 낯설음에 회의 후에 혼자 전임의 실에서 공부도 하고 하였지만, 처음 발디디는 영역이라 혼자 답답해 했었습니다.

하지만, 그 동안 의과학자로서, 임상 진료를 하는 의사로서, 후배들을 지도해주시는 지도자로서 교수님의 열정과 애정을 가까이에서 지켜볼 수 있었던 것과, 제가 전공의 과정부터 석사과정까지 김미금 교수님께 지도를 받을 수 있었던 것은 제 인생의 커다란 선물이라고 생각합니다.

595 이 연구를 더욱 더 다듬어 질 수 있게 연구 계획과 논문 심사의 위원장을 맡아
596 주시고 명철한 제안과 배려를 해주신 현준영 교수님께 무한한 감사의 말씀
597 드립니다. 또한 연구의 목적을 명확히 잡아주시고, 추가적인 분석에 대한 조언을
598 아낌없이 주신 송현범 교수님께도 깊은 감사의 말씀 드립니다.
599 안구 표면 에서의 수지상 세포의 역할 및 분포는 아직 많이 알려져 있는 분야가
600 아니며, 짧은 기간에 한 두명으로 진행될 수 있는 연구가 아닙니다. 저희 연구실의
601 기틀을 잡아주신 위원량 교수님, 안과 연구실을 지지해 주신 박기호 과장님, 제게
602 실험을 알려주신 최혁진, 오주연, 윤창호 교수님께 감사의 말씀 드립니다. 또한 실
603 험을 곁에서 같이 진행하고 도와준 류진숙 선생님께 감사의 말씀 드립니다.